RESEARCH ARTICLE

Rolling with the flow: bumblebees flying in unsteady wakes

Sridhar Ravi[1],*, James D. Crall[1], Alex Fisher[2] and Stacey A. Combes[1]

[1]Department of Organismic and Evolutionary Biology, Harvard University, Cambridge, MA 02138, USA and [2]School of Aerospace, Mechanical and Manufacturing Engineering, RMIT University, Melbourne, VIC 3000, Australia

*Author for correspondence (sravi@fas.harvard.edu)

SUMMARY

Our understanding of how variable wind in natural environments affects flying insects is limited because most studies of insect flight are conducted in either smooth flow or still air conditions. Here, we investigate the effects of structured, unsteady flow (the von Karman vortex street behind a cylinder) on the flight performance of bumblebees (*Bombus impatiens*). Bumblebees are 'all-weather' foragers and thus frequently experience variable aerial conditions, ranging from fully mixed, turbulent flow to unsteady, structured vortices near objects such as branches and stems. We examined how bumblebee flight performance differs in unsteady *versus* smooth flow, as well as how the orientation of unsteady flow structures affects their flight performance, by filming bumblebees flying in a wind tunnel under various flow conditions. The three-dimensional flight trajectories and orientations of bumblebees were quantified in each of three flow conditions: (1) smooth flow, (2) the unsteady wake of a vertical cylinder (inducing strong lateral disturbances) and (3) the unsteady wake of a horizontal cylinder (inducing strong vertical disturbances). In both unsteady conditions, bumblebees attenuated the disturbances induced by the wind quite effectively, but still experienced significant translational and rotational fluctuations as compared with flight in smooth flow. Bees appeared to be most sensitive to disturbance along the lateral axis, displaying large lateral accelerations, translations and rolling motions in response to both unsteady flow conditions, regardless of orientation. Bees also displayed the greatest agility around the roll axis, initiating voluntary casting maneuvers and correcting for lateral disturbances mainly through roll in all flow conditions. Both unsteady flow conditions reduced the upstream flight speed of bees, suggesting an increased cost of flight in unsteady flow, with potential implications for foraging patterns and colony energetics in natural, variable wind environments.

Key words: bumblebee flight, flight stability, von Karman street, unsteady flows, turbulence.

Received 13 May 2013; Accepted 12 August 2013

INTRODUCTION

Volant insects employ a variety of unsteady fluid-mechanic phenomena to remain airborne, including leading edge vortex generation (Ellington et al., 1996), wake capture during hovering (Dickinson et al., 1999), rotational circulation during pronation and supination (Dickinson et al., 1999), and reduction of the Wagner effect *via* clap and fling (Miller and Peskin, 2009). Over the past two decades, our understanding of these phenomena has been significantly improved by studies exploring the flow field over insect wings in free and/or tethered flight conditions, and through the use of dynamically scaled robotic models (for reviews, see Sane, 2003; Wang, 2005). Nearly all experiments on insect flight aerodynamics have been conducted within the confines of laboratories, in the absence of external flow (i.e. still air) or in very smooth flow produced by laminar wind tunnels. However, the vast majority of insects reside in the outdoor environment, within the atmospheric boundary layer (ABL) that extends to a few hundred meters above the Earth's surface, where atmospheric properties (wind, temperature, humidity, etc.) are significantly influenced by the terrain (Stull, 1988). Though migrating insects routinely fly at much higher altitudes (>1000 m) and are assisted by large-scale meteorological events, these insects too descend to the surface layer for tasks such as feeding, resting and mating (see Drake and Farrow, 1988; Chapman et al., 2011).

Flight within this region of the atmosphere can be challenging, even in wind-free conditions, because the Earth's surface is seldom flat, and it contains numerous natural and man-made structures that hinder straight, level flight. Wind conditions within the ABL are highly variable, in part because of pressure differences induced by meteorological phenomena and Coriolis forces arising from the Earth's rotation. Excluding extreme weather events, mean wind speeds in the ABL generally vary from $0\,\mathrm{m\,s^{-1}}$ (still air) to $10\,\mathrm{m\,s^{-1}}$ (strong breeze), and wind direction can change rapidly (Stull, 1988). Diurnal insects are further challenged by stronger daytime winds because of convection from the Earth's surface. Some insects may be forced to cease flying in windy weather (Feltwell, 1982; Hendry, 1989; Combes and Dudley, 2009), but many appear to be capable of contending with the adverse effects of strong, variable environmental airflow through active and/or passive flight control strategies (Crall and Combes, 2013). While some recent studies have investigated the effects of large-scale weather phenomena on insect flight, particularly related to long-distance migration (Chapman et al., 2011), the effects of variable wind patterns on insect flight at shorter time scales within the ABL remain virtually unexplored.

The interaction between airflow and the terrain, which imposes obstacles in the wind's path, can result in highly complex and turbulent flow fields (Watkins et al., 2006). While the flow far away from obstacles is generally well mixed and turbulent, flow in the near wake can be significantly different, with objects such as trees,

branches and flowers producing unsteady but structured flow fields similar to those seen in the wake of bluff bodies. Here, we investigate the effects of unsteady, structured flow in the wake of bluff bodies on the flight performance of bumblebees. Bumblebees are ideal subjects for studying the effects of unsteady wind on insect flight, as they continue to forage even in adverse weather conditions (Heinrich, 2004; Crall and Combes, 2013) and thus are likely to experience a wide range of environmental flow conditions.

We measured instantaneous position and orientation of bees as they flew upstream in a wind tunnel through smooth flow, as well as through the unsteady, von Karman vortex street present in the wake of a circular cylinder. The cylinders used to generate unsteady flows may be considered as abstracts of the tree trunks or branches that bees would routinely fly around while foraging in windy weather. We also investigated the effects of the orientation of the flow disturbance by generating flows behind both a vertical and a horizontal cylinder, which induced strong lateral and vertical disturbances, respectively.

Several recent studies have revealed that body orientation and translational motions are tightly coupled in some flying insects [e.g. in both hawkmoths (Dudley and Ellington, 1990) and bumblebees (Willmott and Ellington, 1997), pitch angle is coupled to longitudinal/forward motion]. However, these coupled motions have primarily been examined during voluntary maneuvers such as turning, ascending or accelerating, and therefore reflect active control strategies initiated by the insect. The passive response of flying insects subjected to unexpected aerodynamic disturbances may be very different, and rotational and translational motions may not be coupled in the same way. In addition, the passive responses of insects to external flow disturbances may differ between species, depending on morphology and flight kinematics. For example, honeybees subjected to an isolated gust of wind display large rolling motions, whereas stalk-eye flies subjected to the same disturbance display significant yaw as well as roll (Vance et al., 2013). Identifying the body axes about which insects are least stable to external perturbations, as well as the coupled rotational and translational motions employed during active maneuvering, is a crucial step in understanding how flying insects negotiate complex, natural aerial environments.

We compared the performance of bees flying in smooth and unsteady, structured flow to address three main questions: (1) how does unsteady, structured flow affect the trajectory and flight speed of bumblebees; (2) how does unsteady flow affect the orientation and stability of bumblebees; and (3) do flow disturbances oriented vertically or horizontally produce equivalent responses along the corresponding axes of flying bees?

MATERIALS AND METHODS
Study specimens and flight tests

Bumblebees (*Bombus impatiens* Cresson 1863) from a commercial breeder (BioBest, Ontario, Canada) were maintained in the laboratory and given continuous access to a foraging chamber where they could feed freely from an artificial, purple flower containing linalool-scented nectar. Fourteen individuals of similar size (body length=14±0.5 mm, mass=165 mg ±10%) were selected for flight experiments.

Each bee was isolated from the hive and cold anesthetized, and a marker (discussed below) was affixed to the dorsal surface of its thorax using cyanoacrylate glue. The marked bee was then placed in a transparent chamber (0.4×0.4×0.4 m) and allowed to recover and fly freely, without access to food, for approximately 2 h prior to the experiment.

Once sufficiently starved, each bee was placed in the wind tunnel (with no airflow) where it could feed from an artificial flower resembling the one in the foraging chamber. Once feeding commenced, the bee was allowed to feed for ~10 s, and was then separated from the nectar source and released at the downstream end of the wind tunnel. If the bee did not fly towards the artificial flower, it was manually re-introduced to the nectar source and subsequently separated. This cycle was repeated until the bee flew directly to the nectar source. Once consistent behavior was established, wind was introduced and bees were filmed as they flew upstream through smooth flow or an unsteady flow field. Each bee was flown sequentially in each of the three flow conditions, with the order of flow conditions randomized between individuals.

Experiments were conducted in a 6-m-long suction-type open-return wind tunnel with a 0.9×0.5×0.5 m working section. The wind speed was set to ~2.55 m s^{-1}, which represents an intermediate cruising velocity for bumblebees (Ellington, 1991). To generate structured, unsteady flow, a circular cylinder with a diameter of 25 mm, corresponding to the average wing span of the bumblebees, was placed at the inlet of the test section, extending across the width of the working section. The artificial flower that bees flew towards was positioned within the cylinder in the unsteady trials (Fig. 1A). To maintain behavioral consistency in the smooth flow trials, we attached a small (~5 mm diameter) artificial flower to the upstream mesh of the wind tunnel.

This method of unsteady flow generation gives rise to a von Karman vortex street in the wake of the cylinder (Fig. 1A), and has been employed by a number of researchers examining the influence of unsteady flow on swimming and flying animals (Liao et al., 2003; Beal et al., 2006; also see Ortega-Jimenez et al., 2013). At the chosen velocity, the spatial scales of the vortices emanating from the cylinder are on the order of the wing span of the bees. Although there exists limited understanding of the influence of various scales of unsteady flow structures on flapping flight performance, we hypothesize that disturbances on the order of the bee's wing span would produce the greatest instability; disturbances many orders of magnitude greater would be experienced as quasi-steady changes in oncoming flow, whereas those many orders of magnitude smaller would average out across the body to produce minimal disturbance.

We filmed bees and quantified airflow within a specific interrogation volume (a cube with side lengths of 100 mm, located 100 mm downstream from the cylinder; Fig. 1A). The downstream distance was chosen to avoid the recirculating region in the near wake of the cylinder and to allow the formation of a full von Karman vortex street. Fluctuations in flow velocity within this volume were quantified in the absence of bees, using a three-component hot-wire anemometer sampling at 1 kHz, calibrated against a standard pitot-static tube.

During flight trials, bees were filmed as they flew through the interrogation volume using two Photron SA3 high-speed cameras (San Diego, CA, USA) sampling at 1000 Hz, placed above the wind tunnel at ~30 deg from the vertical. A static calibration cube that filled the volume of interest was used for spatial calibration *via* direct linear transformation (Hedrick, 2008).

Triangular markers were manually placed on the thorax of bees to enable estimation of the bees' position and orientation. The markers consisted of three black points representing the vertices of an isosceles triangle (measuring 2.7×2.3 mm) set upon a white background (Fig. 2B). Footage of the bees in flight revealed that the marker was well removed from the wings and did not interfere with wing kinematics.
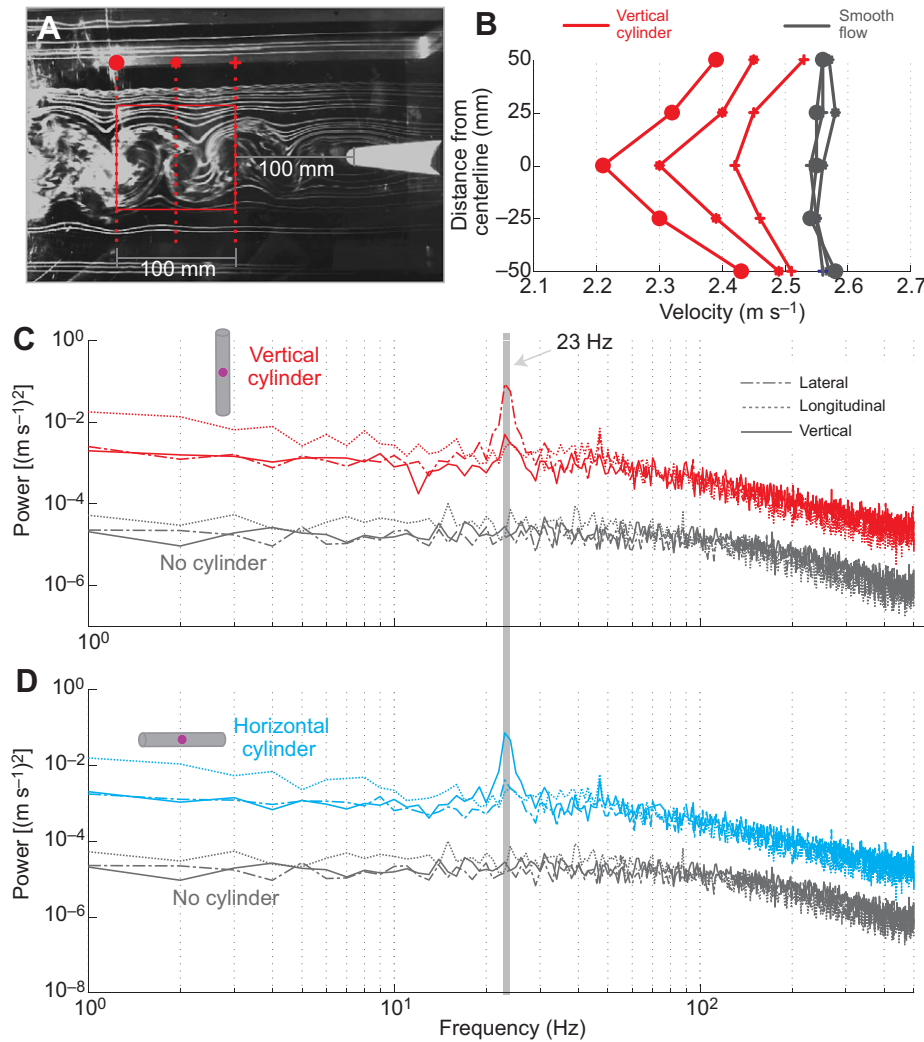
Fig. 1. (A) Smoke flow visualization showing the von Karman vortex street in the wake of the vertical cylinder. Position and orientation of bees was measured within a cube of 100 mm side length, the location of which is depicted by the red square. The purple marker seen in the center of the cylinder represents the artificial flower. (B) Mean wind velocity measured at different locations within the 100 mm cube (locations shown by symbols in A). (C,D) Spectra of velocity fluctuations measured along the three axes in the wake of the vertical and horizontal cylinder, respectively, as well as with no cylinder present.

Kinematic reconstruction and analysis

The recorded flight sequences were digitized using an open-source MATLAB-based routine, DLTdv5 (Hedrick, 2008), utilizing the automated tracking feature to localize the three black points on the triangular marker throughout each sequence. Subsequent analysis of the bee's position and orientation was performed in MATLAB (The MathWorks, Natick, MA, USA). Reconstructed data were filtered with an eighth-order Butterworth low-pass filter with a cutoff frequency of 200 Hz to reduce error due to marker localization (see Error estimation, below). The software utilizes direct linear transformation (DLT) to calculate the location of an arbitrary point in 3D space based on the location of the point on each camera's view. For all flight sequences only the three black points on the marker (Fig. 2B) were digitized.

Mean ground speed of bees was calculated by numerically integrating the absolute flight path of the bee and dividing it by the total flight time. Mean air speed of bees along their flight path was calculated as the sum of the mean wind speed in the interrogation volume and the mean ground speed traveled by the bee:

$$(\text{Mean air speed})_{\text{Tot},x,y,w} = \frac{(\text{Total distance traveled})_{\text{Tot},x,y,w}}{\text{Total time}} + (\text{Mean windspeed})_{\text{Tot},x,y,w} \,. \quad (1)$$

In smooth flow conditions, the mean wind speed was uniform within the interrogation volume; however, in the wake of the cylinder, mean streamwise velocity varied slightly across the control volume (Fig. 1B). Because simultaneous measurement of the bee's position and instantaneous wind speed at that particular position is impractical, we used the mean wind speed across the interrogation volume combined with the bee's ground speed to estimate mean air speed in unsteady flow trials. This method of air speed estimation was considered reasonable because variation in mean wind speed across the interrogation volume was relatively limited, and the flight time of the bees was much greater than the advective time scales of the von Karman vortices.

To further elucidate the influence of unsteady flows on the bees' flight trajectories, ground speeds of bees in the longitudinal, lateral and vertical directions (in a global coordinate system; Fig. 2B) were calculated separately and compared between flow conditions. For all flow conditions there was no mean wind in either the lateral or vertical direction, hence the lateral and vertical airspeeds were equal to their respective ground speeds. Standard deviations of velocity along each axis in each trial were calculated to compare the relative strength of velocity fluctuations along each axis. Power spectra of bee velocity along each axis were calculated using the Welsh method of spectral estimation in MATLAB to identify dominant frequencies of motion. Because bumblebees typically adopt a 'casting' flight path, flying slowly from side to side as they move upstream, we also examined the standard deviations of velocities subjected to a 3 Hz high-pass filter to separate the higher-frequency components
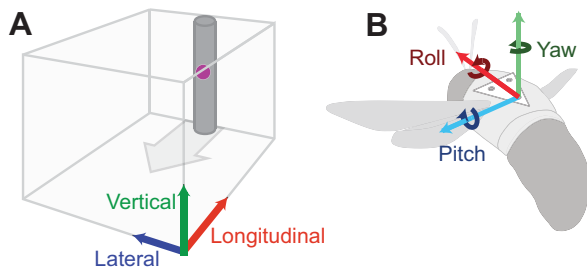
Fig. 2. (A) Global coordinate system used for measurements of the position of bees. (B) Local coordinate system used for measurements of the body orientation of bees.

of the bees' velocity fluctuations from the low-frequency casting behavior. The cutoff frequency of 3 Hz was chosen arbitrarily, based on the power spectra of bee velocity; however, sensitivity to cutoff frequency was evaluated, and the filtered results were found to be relatively insensitive to cutoff frequency over a range of ~3–10 Hz.

Instantaneous acceleration was calculated by numerically differentiating bee velocity. Power spectra of accelerations along the longitudinal, lateral and vertical axes were calculated to assess dominant frequencies of acceleration fluctuations and standard deviations of accelerations were calculated to compare the magnitude of fluctuations along the three axes.

The influence of flow conditions on the body orientation and rotation rates of bees was assessed by evaluating variation in roll, pitch and yaw angles of the triangular markers using a rigid body assumption. As abdomen position was not tracked in the flight sequences, pitch angle estimation through the conventional method (angle between head–abdomen vector and horizon) could not be made; however, because most aerodynamic force is produced in the thorax and many insects are known to actuate their abdomens independently during flight, we chose to use the orientation of the thorax itself for pitch angle estimation. To calculate the instantaneous orientation of the thorax, a local plane was constructed based on the three points on the triangular marker. The origin of the right-handed local coordinate system of the plane was placed on the posterior-most point on the marker and translational components between the local and global coordinate systems were removed (see Fig. 2B). Subsequently, the directional cosine matrix (DCM; i.e. the rotation matrix between the local and global coordinate systems) was calculated. From the DCM, the Euler angles based on the roll–pitch–yaw (RPY) sequence of intrinsic rotations was obtained (Diebel, 2006). Conceptually, the RPY angles derived from this method imply that the instantaneous orientation of the marker (bee) with respect to the neutral position (where the local and global coordinate systems are coincident), can be described by initially performing a rotation about the local coordinate x-axis (roll), subsequently a rotation about the local coordinate y-axis (pitch) and finally a rotation about the local coordinate z-axis (yaw). A similar method was used by Walker et al. (Walker et al., 2012) and Nicholas (Nicholas, 2012) to estimate the orientation of freely flying hoverflies and houseflies, respectively.

Power spectra of orientation angles were calculated to identify dominant frequencies of fluctuations in body rotation around the roll, pitch and yaw axes. To obtain instantaneous rotation rates of bees in the local coordinate system, the time derivative of the RPY angles was multiplied by the rotation rate matrix (Diebel, 2006). Mean absolute rotation rates were calculated from the instantaneous angular velocity data. The rotation data were also treated with a 3 Hz high-pass filter to remove low-frequency casting motions, as in the translational analyses described above.

To understand how body rotations (either voluntary or involuntary) are related to translational motions of bees, we performed normalized cross-correlation analysis between instantaneous roll/yaw angles and lateral acceleration, as well as between pitch angle and vertical/longitudinal accelerations.

Statistical significance of results was analyzed by performing paired t-tests (N=14 individuals in all cases) between experimental conditions [smooth flow (S), unsteady wake of horizontal cylinder (U_{horiz}) and unsteady wake of vertical cylinder (U_{vert})] in MATLAB.

Error estimation

Digitization error in localizing the centroids of marker points is expected to be on the order of 1–2 pixels, which is much smaller than the mean number of pixels separating the markers (~30). This error is expected to manifest only at higher frequencies, on the order of the Nyquist frequency. The digitized data were passed through an eighth-order Butterworth low-pass filter to remove any higher-frequency errors due to the digitization process, with a cutoff frequency of 200 Hz, which is lower than the Nyquist frequency (500 Hz) but higher than the flapping frequency of the bees (~180 Hz).

Error caused by the 3D reconstruction process was analyzed using the DLTdv5 MATLAB routine, which provides residuals (in pixels) from the direct linear transformation performed for each time instant (Hedrick, 2008). These residuals are the root mean square error in the 3D reconstruction of the points from the camera views, and may be considered a metric for the accuracy of the digitization process. A low residual is indicative of accurate triangulation of the points in 3D space. To avoid errors in estimation of orientation angles because of the relatively close proximity of points on the marker, only sections of flight sequences with DLT residuals <2 pixels were chosen for further analysis. To further assess the accuracy of the reconstruction process, the reconstructed distances between marker points were compared with the actual physical distances between them for each time instant analyzed. For the flight sequences analyzed (those with DLT residuals <2), the root mean square difference between reconstructed and actual marker distances was <0.05 mm, corresponding to an uncertainty of <2%.

Markers were affixed to each bee's thorax manually, and thus may have been offset from the bee's neutral axes by different amounts in the 14 individuals tested. These offsets in marker positioning could introduce error into the estimation of instantaneous body orientation angles. However, the output variables used for statistical analysis (standard deviation of rotation angles, mean absolute rotation rates, standard deviation of rotation rates, etc.) were based on changes in orientation angle, and thus are not affected by slight errors in estimation of actual body orientation angles.

RESULTS
Flow conditions

With unimpeded (smooth) flow, a flat velocity profile was present across the interrogation volume (<2% variation in mean flow speed; Fig. 1B) and turbulence intensity (standard deviation/mean wind speed) was less than 1.2%. There were no dominant velocity fluctuations at any particular frequency (Fig. 1C,D), indicating that the flow disturbance created by the small flower embedded in the upstream mesh was minimal.

When either a horizontal or vertical cylinder was introduced to generate unsteady flow, a deficit in mean longitudinal velocity could be seen in the wake of the cylinder (as compared with the smooth

flow), and the mean velocity profile varied slightly throughout the interrogation volume (Fig. 1B). Vortex shedding occurred at 23 Hz (Fig. 1C,D), in agreement with the predicted vortex shedding Strouhal number of 0.19 (Roshko, 1961; Vickery, 1966). When the cylinder was aligned vertically, strong lateral velocity fluctuations were induced at the shedding rate (Fig. 1C), and when the cylinder was aligned horizontally, strong vertical velocity fluctuations were induced (Fig. 1D). Because of the influence of the counter-rotating vortices, velocity along the dominant axis of disturbance (i.e. lateral flow with the vertical cylinder, vertical flow with the horizontal cylinder) varied approximately as a square wave. Smaller velocity fluctuations in the non-dominant directions at 23 Hz can also be seen in the spectra (Fig. 1C,D), indicating that some 3D effects were present; these may be attributed to ambient free-stream turbulence within the tunnel and small surface non-uniformities of the cylinder.

Flight speed and trajectory

Mean air speed of bees along their flight trajectory was lower in unsteady flow as compared with smooth flow conditions (paired t-tests: S–U_{horiz} and S–U_{vert}, $P \ll 0.0001$; Fig. 3), but did not differ with orientation of the cylinder (U_{horiz}–U_{vert}, $P = 0.55$). Similarly, longitudinal (upstream) air speed was lower in unsteady flow than in smooth flow, but did not differ with flow orientation (S–U_{horiz} and S–U_{vert}, $P \ll 0.0001$; U_{horiz}–U_{vert}, $P = 0.6533$). There were no significant differences in mean longitudinal and lateral ground speed among flow conditions (Fig. 4A,B), but mean vertical ground speed was higher in the wake of the horizontal cylinder as compared with the other two flow conditions (S–U_{horiz}, $P = 0.035$; U_{horiz}–U_{vert}, $P = 0.04$; S–U_{vert}, $P = 0.75$; Fig. 4C).

Standard deviations of longitudinal, lateral and vertical velocity were similar across all three flow conditions (S–U_{horiz}, $P = 0.5$, 0.4 and 0.4 for longitudinal, lateral and vertical directions, respectively; S–U_{vert}, $P = 0.2$, 0.8 and 0.3; U_{horiz}–U_{vert}, $P = 0.8$, 0.5 and 0.9; Fig. 4G–I, solid boxes). However, the flight trajectories of bees flying upstream in the wind tunnel consisted of motions over a range of frequencies. Bees typically displayed high-amplitude, low-frequency casting movements while flying upstream; these smooth, low-frequency motions were less pronounced in unsteady flows, where higher frequency movements around the flight path were more common (Fig. 5). When the low-frequency casting maneuvers were removed by a 3 Hz high-pass filter, the standard deviation of lateral velocity differed significantly between flow conditions, with larger lateral velocity fluctuations in both unsteady flow conditions as compared with smooth flow (S–U_{horiz}, $P = 0.02$; S–U_{vert}, $P < 0.001$; U_{horiz}–U_{vert}, $P = 0.002$; Fig. 4H, open boxes), and the highest lateral fluctuations were generated by the vertical cylinder. Standard deviations of filtered longitudinal and vertical velocity data remained similar across flow conditions.

These large fluctuations in lateral velocity at higher frequencies were also manifested as large fluctuations in lateral acceleration under unsteady flow conditions, with the standard deviation of lateral accelerations being highest in the wake of the vertical cylinder (S–U_{horiz}, $P < 0.001$; S–U_{vert}, $P < 0.001$; U_{horiz}–U_{vert}, $P < 0.001$; Fig. 6B). Vertical acceleration fluctuations were generally lower than lateral ones, but the standard deviation of vertical accelerations was significantly higher in unsteady flow generated by the horizontal cylinder than in the other two flow conditions (S–U_{horiz}, $P = 0.006$; S–U_{vert}, $P = 0.20$; U_{horiz}–U_{vert}, $P = 0.03$; Fig. 6C). Acceleration fluctuations in the longitudinal direction were relatively low, with significantly higher fluctuations in the wake of the vertical cylinder as compared with smooth flow (S–U_{horiz}, $P = 0.36$; S–U_{vert}, $P = 0.01$; U_{horiz}–U_{vert}, $P = 0.09$; Fig. 6A).
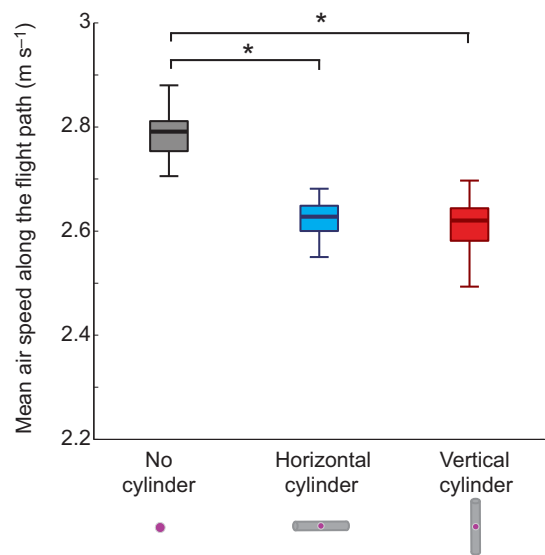

Fig. 3. Mean air speed of bees (N=14) along their flight trajectories in the three flow conditions. Asterisks indicate significant differences (*P<0.05) between treatments.

Spectral analysis revealed peaks in body acceleration near the vortex shedding frequency in both unsteady flow conditions (Fig. 6D–F), similar to the velocity spectra (Fig. 4D–F). However, whereas velocity fluctuations occurred primarily along either the lateral or vertical axis, depending on the orientation of unsteady flow (Fig. 4D–F), acceleration fluctuations near the shedding frequency occurred along all three axes in both unsteady flow conditions (Fig. 6D–F).

Body orientation

As seen previously in standard deviations of bees' velocities (Fig. 4G–I), the standard deviations of bees' orientation angles were also affected by the low-frequency casting maneuvers that bees performed while flying upwind (Fig. 5), leading to similar magnitude of roll and yaw fluctuations in the three flow conditions (S–U_{horiz}, $P = 0.2$ and 0.4 for roll and yaw, respectively; S–U_{vert}, $P = 0.8$ and 0.8; U_{horiz}–U_{vert}, $P = 0.2$ and 0.4; Fig. 7A–C, solid boxes). The pitch angle fluctuations were higher in both unsteady flow conditions as compared with smooth flow (S–U_{horiz}, $P = 0.04$; S–U_{vert}, $P = 0.01$; U_{horiz}–U_{vert}, $P = 0.5$; Fig. 7B, solid boxes, significance bars not shown). However, when low-frequency casting motions are removed with a 3 Hz high-pass filter, it becomes clear that bees experience significantly more high-frequency roll fluctuations in both unsteady flow conditions as compared with smooth flow (S–U_{horiz}, $P \ll 0.0001$; S–U_{vert}, $P \ll 0.0001$; U_{horiz}–U_{vert}, $P = 0.1$; Fig. 7A, open boxes). Differences in pitch and yaw fluctuations were also significant between unsteady and smooth flow conditions (S–U_{horiz}, $P = 0.001$ and 0.002; S–U_{vert}, $P = 0.007$ and 0.02; Fig. 7B,C), but not between unsteady flow conditions (U_{horiz}–U_{vert}, $P = 0.4$ and 0.5; Fig. 7B,C).

Distinct peaks in roll fluctuations (as well as lesser peaks in yaw and pitch) near the vortex shedding frequency were present in the wake of the vertical cylinder (Fig. 7D–F), demonstrating that this unsteady flow pattern destabilized bees, particularly around the roll axis. Surprisingly, no clear peaks in pitching or other body rotations were present in the wake of the horizontal cylinder (Fig. 7D–F), despite the presence of peaks in the vertical air speed of bees (Fig. 4D–F). Spectra of rotation rates (not shown) were similar to those of the orientation angles themselves.
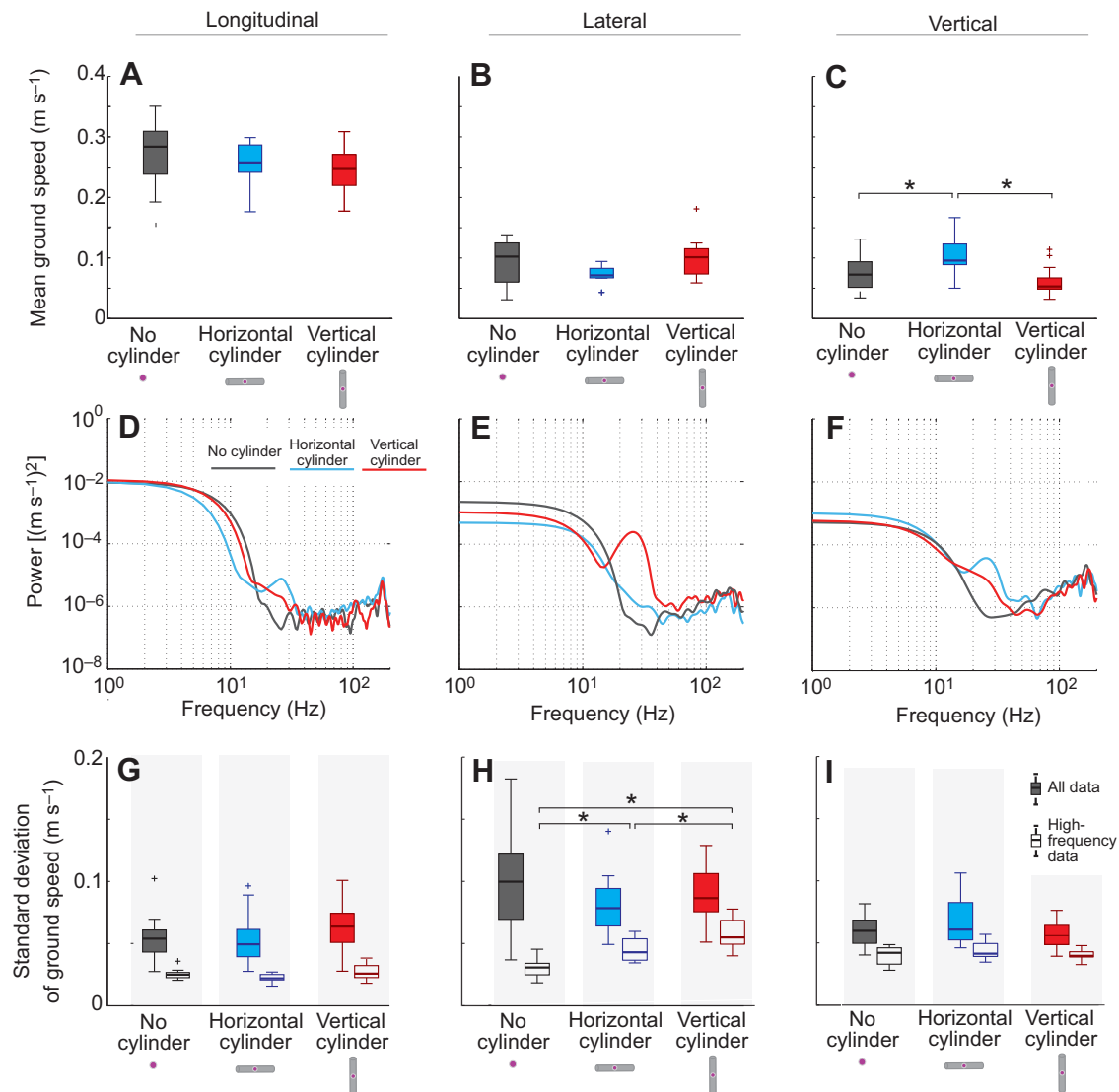
Fig. 4. (A–C) Mean ground speed of bees (*N*=14) along the longitudinal, lateral and vertical axes of the wind tunnel in the three flow conditions. For B and C, mean lateral and vertical ground speed was equal to the mean air speed along those axes. (D–F) Power spectral density of an individual bee's velocity along each axis in the different flow conditions. (G–I) Standard deviation of the bees' velocities along each axis; data for full flight trajectories are shown by solid boxes, and those derived from only higher-frequency motions (3 Hz high-pass filtered data) by open boxes. Asterisks indicate significant differences (*P<0.05) between treatments; plus signs are outliers within a treatment.

Variations in mean (absolute) rotation rates indicated that much higher rotation rates occurred around the rolling axis as compared with pitch or yaw in all three flow conditions (Fig. 8A–C). Mean rolling rates in excess of 500 deg s^{-1} were commonly experienced by the bees in unsteady conditions. Rolling rates were significantly higher in both unsteady flow conditions as compared with smooth flow, and were higher behind the vertical cylinder as compared with the horizontal one (S–U_{horiz}, P<<0.0001; S–U_{vert}, P<<0.0001; U_{horiz}–U_{vert}, P=0.003; Fig. 8A). Pitching rates were much lower than rolling rates, but bees pitched more quickly in unsteady as compared with smooth flow (S–U_{horiz}, P=0.001; S–U_{vert}, P=0.0001; U_{horiz}–U_{vert}, P=0.7; Fig. 8B), and yawing rates were the lowest, but were still significantly higher in unsteady flow (S–U_{horiz}, P=0.004; S–U_{vert}, P=0.0002; U_{horiz}–U_{vert}, P=0.2). The standard deviation of rotation rates (Fig. 8D–F) was generally higher than the absolute mean, but variations between smooth and unsteady conditions were similar, with all flow conditions producing the largest fluctuations around the roll axis, followed by pitch and yaw.

Relationships between body orientation and translational acceleration

The kinematic analyses revealed a strong cross-correlation (with zero phase lag) between roll angle and acceleration along the lateral axis of the wind tunnel for bees in smooth flow (r=0.7±0.2, N=14 bees; Fig. 9A,B), whereas there was no clear correlation between yaw angle and lateral acceleration (r=0.3±0.3). The r-values indicate the mean correlation coefficients (±95% confidence intervals) across all individuals; all correlations were statistically significant (P<0.001). As expected for voluntary maneuvers (in which a body rotation redirects the axis of force production, leading to translation), the correlation between roll angle and lateral acceleration in smooth flow was positive, with the largest lateral accelerations coinciding with the largest roll angles (Fig. 9A).

In contrast, there was no substantial correlation between roll angle and lateral acceleration during trials conducted in unsteady flow generated by the vertical cylinder (Fig. 9B). However, when the data were filtered with a 3 Hz low-pass filter to remove higher-frequency
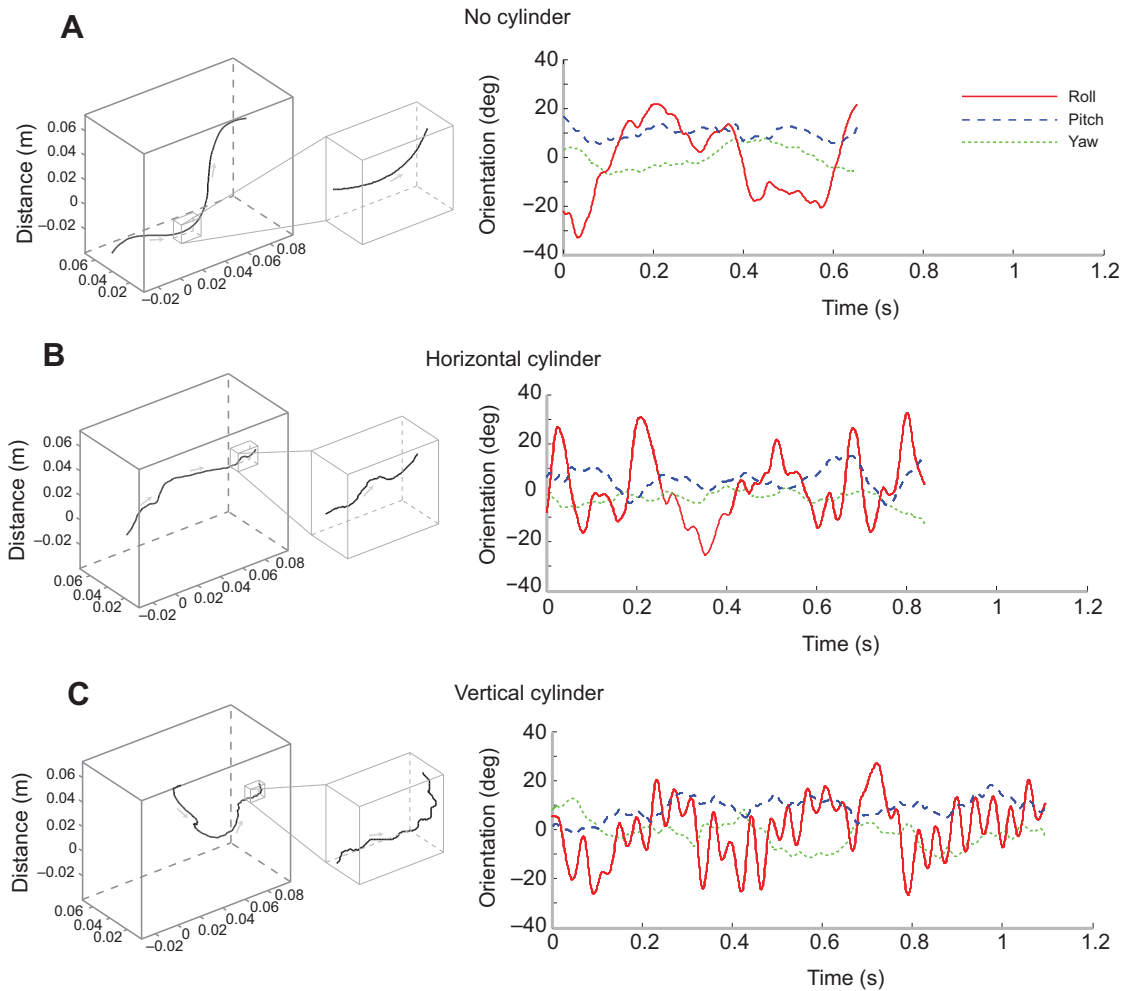
Fig. 5. (A–C) Typical flight trajectories and body orientations of a bee in each flow condition. The 3 day trajectory (in cm) within the wind tunnel is shown on the left, with movements within the interrogation volume shown by the inset. Instantaneous roll, pitch and yaw while flying through the interrogation volume is shown on the right.

motions (in contrast to previous filtering that excluded low-frequency motions), the correlation between roll angle and lateral acceleration again became positive and significant ($r=0.7\pm0.15$; Fig. 9C). The same pattern was generally true for flight in unsteady flow generated by the horizontal cylinder (unfiltered: $r=0.2\pm0.3$; filtered: $r=0.6\pm0.2$).

The correlation between pitch angle and vertical acceleration was relatively low but positive in smooth flow ($r=0.2\pm0.2$). In unsteady flow, there was no clear correlation between pitch angle and vertical acceleration (horizontal cylinder: $r=0.1\pm0.5$; vertical cylinder: $r=0.0\pm0.2$), and filtering with a 3 Hz low-pass filter did not significantly alter this relationship (horizontal cylinder: $r=0.0\pm0.3$; vertical cylinder: $r=0.3\pm0.4$).

DISCUSSION
Effects of unsteady flow on flight trajectory and stability
In the broader context of insect flight in natural environments, one of the key questions is how well bumblebees are able to contend with unsteady airflow; ultimately, we would like to know how bees' capabilities compare both with other flying insects, as well as with the magnitude of unsteady flows that bees experience in the real world. As compared with the null hypothesis that bees would display translational and rotational fluctuations equal to those present in the

external flow (i.e. if they were massless and had no active or passive control of their position or orientation), it is clear that bees are quite successful overall at attenuating external flow perturbations (note that for the unsteady flow conditions, only fluctuations at frequencies >3 Hz were considered, in order to remove the effects of voluntary casting behavior; Table 1). Bees typically displayed fluctuations (i.e. standard deviations) in translational velocity and acceleration that were at least an order of magnitude less than those present in the external flow, and showed similar levels of attenuation in pitch and yaw angles.

Some attenuation of the fluctuations induced by the flow is expected because the bee's mass (inertia) will passively reduce the magnitude of fluctuations experienced by the bee. However, bees are undoubtedly also responding actively to minimize and correct for external perturbations through changes in wing kinematics, as has been shown in honeybees and other flying insects responding to isolated external perturbations (Vance et al., 2013; Ristroph et al., 2013). Active responses of the bees could not be determined in this study because of the lack of information on wing kinematics. Even with this information, it would be difficult to conclusively identify the extent of active response, because of the tight coupling between disturbance and response, as well as the complex spatial and temporal variation in external flows. The rapid drop-off in
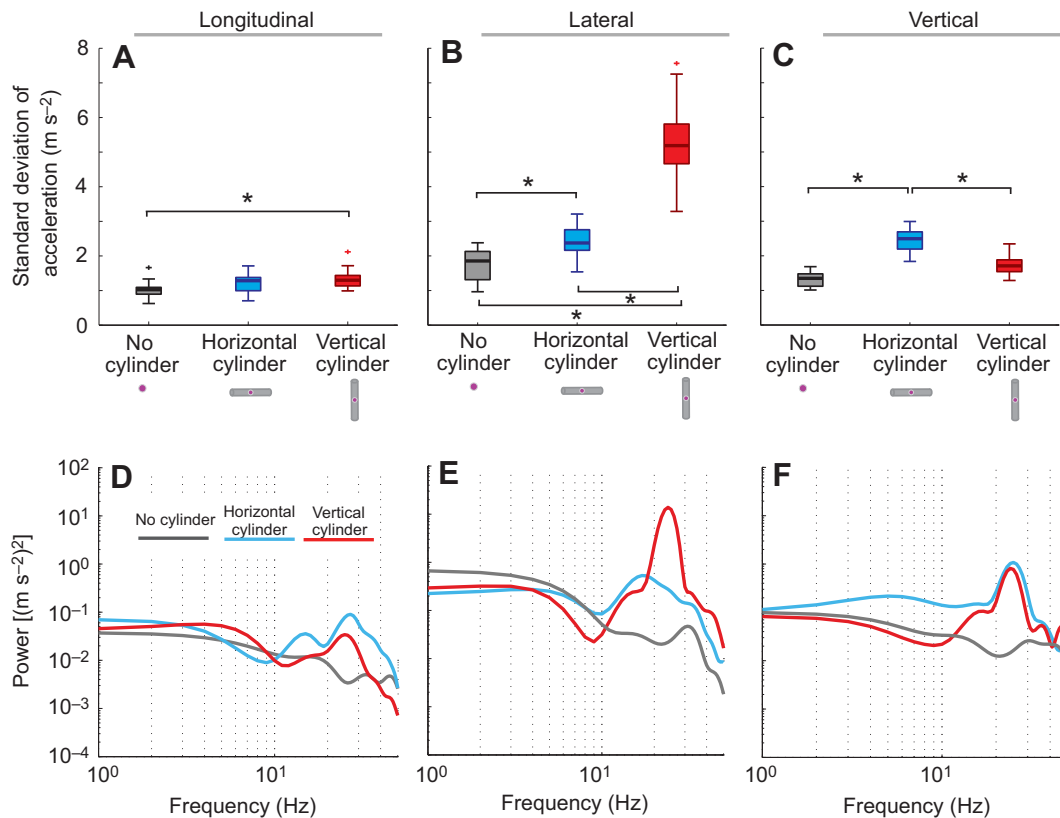
Fig. 6. (A–C) Standard deviation of bees' accelerations along the longitudinal, lateral and vertical axes of the wind tunnel in the three flow conditions. (D–F) Power spectral density of an individual bee's acceleration along each axis in the different flow conditions. For analysis of accelerations, data were passed through a 50 Hz low-pass filter. Asterisks indicate significant differences (*$P<0.05$) between treatments; plus signs are outliers within a treatment.

energy of acceleration fluctuations at frequencies higher than the vortex shedding rate (Fig. 6) suggests that the bees did not respond to disturbances induced by the vortices with rapid corrective accelerations, but rather responded at rates commensurate with the disturbances.

While bees can clearly attenuate external perturbations along all axes (Table 1), they appear to be less sensitive (i.e. more stable) to perturbations along the vertical axis, as opposed to the lateral axis. Fluctuations in vertical acceleration in response to the horizontal cylinder were approximately half the magnitude of fluctuations in lateral acceleration in response to the vertical cylinder (Fig. 6), and the energy present at the vortex shedding frequency in the spectra is significantly higher in the latter. This could imply that bees are more aerodynamically stable along the vertical axis and/or that they are more adept at actively responding to translational disturbances along this axis. However, the lower magnitude of fluctuations in pitch as compared with roll under all flow conditions (Fig. 8) suggests that bees may be 'passively' more immune to disturbances along the vertical/pitching axis. In addition, the presence of a peak in vertical ground speed fluctuations near the vortex shedding frequency in the wake of a horizontal cylinder, but the absence of a peak in pitching, suggests that the von Karman street arising from the horizontal cylinder resulted only in translational perturbations along the vertical axis, and did not cause any rotational disturbances or elicit rotational responses in bees at the vortex shedding frequency.

Apart from the passive attenuation of disturbances by virtue of body mass (inertia) and other damping phenomena [e.g. translational damping by virtue of flapping kinematics, and rotational damping because of flapping counter torque (Hedrick, 2011)], as well as active

responses in the form of wing kinematic modulation, bumblebees likely employ a variety of other active and passive means to resist perturbations and maintain stability in unsteady flows. Active deflection of various body parts has been shown to influence stability, such as in orchid bees that extend their limbs when flying in turbulent air to increase their rolling moment of inertia (Combes and Dudley, 2009). Other studies have shown that abdominal deflection may augment not only pitching stability, but also translational stability along the vertical axis (Dyhr et al., 2013). Though no obvious leg extension occurred in the flight sequences collected for this study, some abdominal deflection was noted qualitatively, which could contribute to the bees' stability along the vertical/pitching axis.

The relatively limited sensitivity to disturbances along both the vertical and longitudinal axes in comparison to the lateral axis could also arise from the fact that forces are actively produced by the bee along these axes (lift and thrust, respectively). In steady level flight, as the bee counteracts its drag by generating thrust (longitudinal axis) and counteracts its weight by generating lift (vertical axis), a disturbance along these axes will only require a slight modulation of the existing forces to correct for the influence of the disturbance. However, a disturbance along the lateral axis would be expected to have a greater influence, as no (or very limited) forces are being produced along this axis, unless the bee is performing a turning maneuver. Hence, in the case of a lateral disturbance, the bee would need to correct for the disturbance through inertial reorientation (roll) of its primary force vector.

In addition to inherent differences in force production, the rotational moment of inertia of the bee also varies about its three
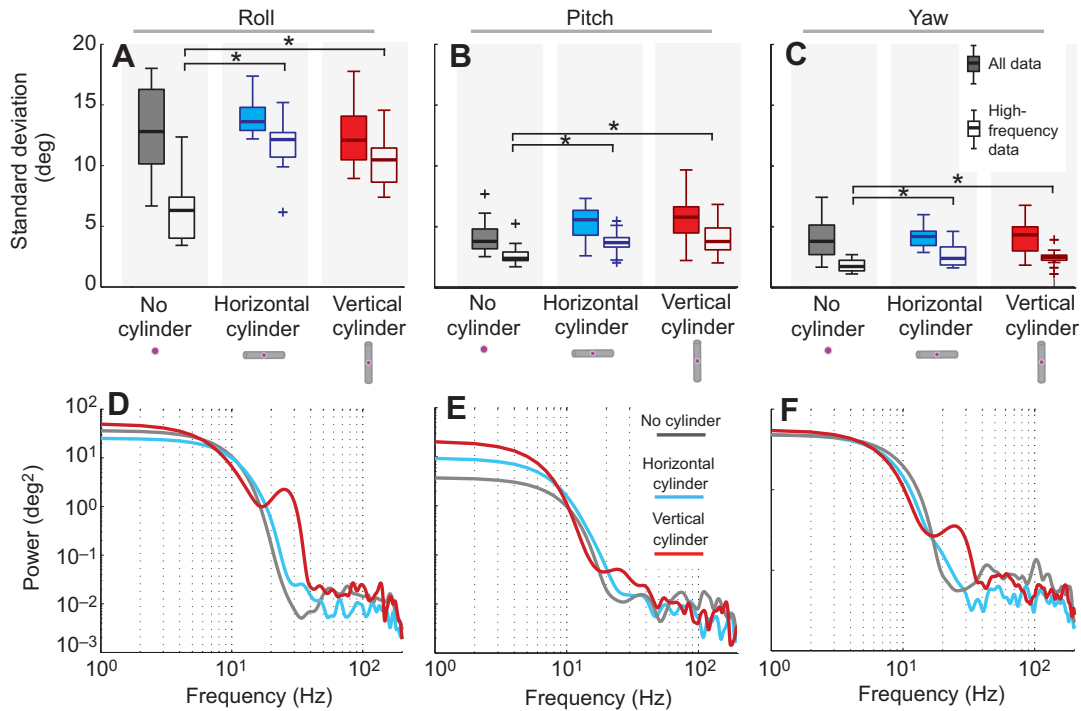
Fig. 7. (A–C) Standard deviation of bees' orientation angles along each body axis (full data set shown by solid boxes and higher-frequency/3 Hz high-pass filtered data by open boxes). (D–F) Power spectral density of the roll, pitch and yaw angles of an individual bee in the three flow conditions. Asterisks indicate significant differences (*P<0.05) between treatments; plus signs are outliers within a treatment.

axes. The rotational moment of inertia is generally lowest around the roll axis, followed by the pitch and yaw axes (Dudley, 2002), and the differences in rotational fluctuations that bees experienced around these axes in unsteady flow follow this trend. Bees rolled far more than they pitched or yawed in all flow conditions, and unsteady flow amplified these trends (Figs 7, 8). Bees also experienced significantly greater fluctuations in velocity and

acceleration along the lateral axis (Figs 4, 6) with external flow perturbations generated by the vertical cylinder imposing lateral forces of over half the bees' body weight (Fig. 6B). Intriguingly, our results vary substantially from parallel experiments on the flight stability of hawkmoths (*Manduca sexta*) (Ortega-Jimenez et al., 2013), which experienced greater fluctuations in yaw than in roll when flying in the wake of a vertical cylinder. It is possible that
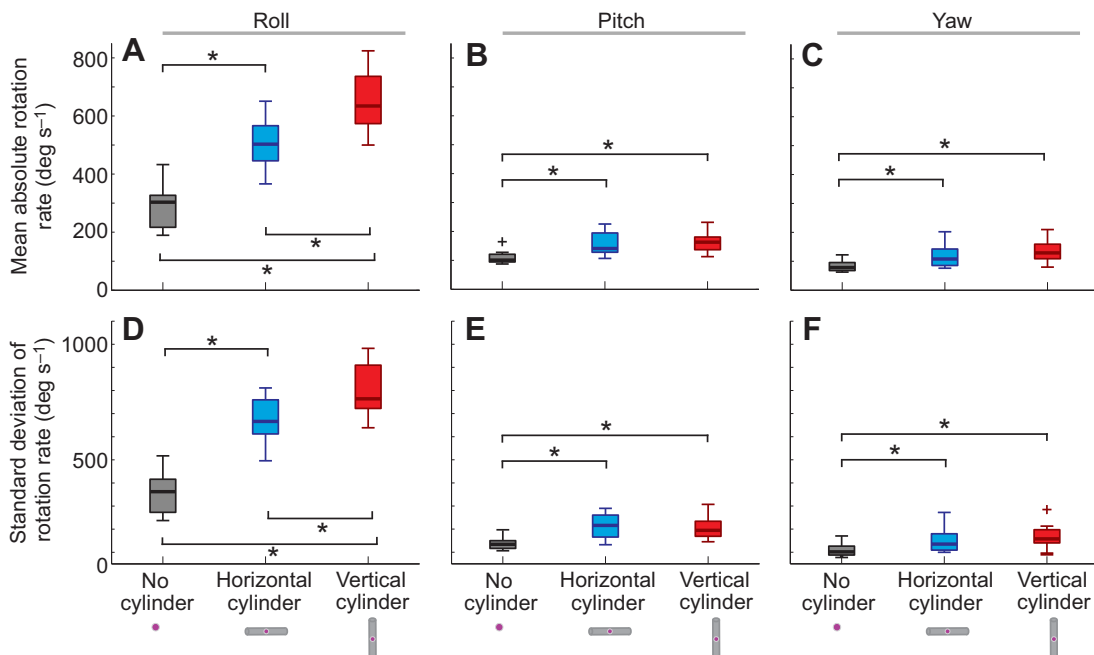

Fig. 8. (A–C) Mean absolute rotation rates of bees, and (D–F) standard deviation of rotation rates in each flow condition. Asterisks indicate significant differences (*P<0.05) between treatments; plus signs are outliers within a treatment.
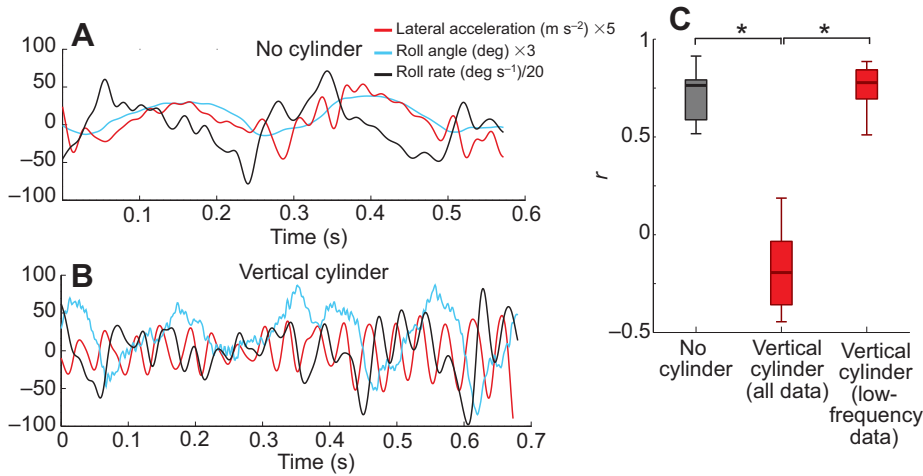
Fig. 9. Time series of the lateral acceleration, roll angle and rolling rate of an individual bee in the no cylinder (A) and vertical cylinder (B) conditions. Note that ordinate scales are different in A and B. (C) The zero-time-shift correlation between roll angle and lateral acceleration of bees (N=14) in smooth flow (left), in the wake of the vertical cylinder (center), and in the same wake with higher-frequency motions removed through filtering (right). Asterisks indicate significant differences (*P<0.05) between treatments.

the differences in observations are due to experimental conditions; bees in our experiment were actively flying upsteam to a food source, whereas hawkmoths were maintaining stationary position at a flower in an oncoming flow. The observed differences may also reflect differences in passive stability or flight control strategy, as these species vary significantly in morphology, wing loading and flapping frequency (Ellington, 1984).

The spectral and temporal analysis of the flight trajectories allowed us to discern that bees typically perform voluntary, lateral casting motions at low frequencies (Fig. 5), and that they primarily utilize the roll axis to perform these lateral maneuvers. Thus, although bees may be more sensitive to disturbances along the lateral/roll axis, they also appear to be most agile around this axis. Bees may make use of the relative ease of perturbing stable flight (i.e. for a given amount of torque, a larger roll can be produced as compared with pitch or yaw) to effect voluntary maneuvers. Similarly, in unsteady flow we would expect that, although bees experience the largest translational perturbations around the lateral axis, they would also be capable of responding most quickly and easily by producing a corrective roll in the opposite direction. This may help explain the relatively low, negative correlation observed between roll and lateral acceleration over the entire frequency range (Fig. 9C); this likely reflects a combination of low-frequency, voluntary casting maneuvers (with positive correlation; Fig. 9C), external perturbations producing lateral acceleration and roll in the same direction (positive correlation), and corrective maneuvers consisting of rolls in the opposite direction (negative correlation).

The lack of a strong correlation between yaw angle and lateral acceleration further reinforces the idea that bees primarily utilize the roll axis for lateral maneuvers (voluntary or corrective). In terms of vertical maneuvers, the low, positive correlation between pitch and vertical acceleration suggest that bees only partially utilize inertial reorientation (i.e. pitch) to regulate vertical motion, and likely also employ other mechanisms, such as altering the magnitude of mean force production through changes in wing kinematics.

Effects of unsteady flow on energetics and cost of flight
One strategy that fish have been shown to adopt for maintaining position and conserving energy in unsteady flows is known as Karman gaiting (Liao et al., 2003). The passive and active compliance of the body to oncoming vortices results in a swaying and/or undulating motion that enables fish to maintain stable position with minimal energetic cost in highly unsteady flow conditions (Liao, 2007). The large differences in morphology and force production mechanisms between laterally undulating fish and flying bees suggests that the interaction of these animals with the oncoming vortices would be considerably different; hence strategies employed by fish may not be suitable (or even feasible) for bees. There is, however, a possibility that bees could actively slalom around oncoming vortices, thereby reducing their energy expenditure. However, this cannot be ascertained in the absence of information regarding the instantaneous position of the vortex with respect to the bee, for which additional experiments combining simultaneous quantitative flow visualization and bee flight path measurements would be required.

Table 1. Summary of the standard deviations of velocity, acceleration and rotation along each axis, in the oncoming flow as compared with in bees

	Smooth flow (no cylinder)		Horizontal cylinder		Vertical cylinder	
	Flow	Bees	Flow	Bees	Flow	Bees
Longitudinal velocity (m s^{-1})	0.065	0.02±0.005	0.31	0.02±0.005	0.32	0.03±0.007
Lateral velocity (m s^{-1})	0.056	0.03±0.01	0.3	0.043±0.01	0.69	0.056±0.01
Vertical velocity (m s^{-1})	0.061	0.04±0.007	0.71	0.046±0.005	0.29	0.042±0.005
Longitudinal acceleration (m s^{-2})	7.1	1.2±0.02	51.6	1.6±0.05	50.5	1.7±0.05
Lateral acceleration (m s^{-2})	4.9	1.6±0.4	102.2	2.7±0.5	49.5	5.2±0.7
Vertical acceleration (m s^{-2})	5.3	1.1±0.1	47.9	2.5±0.2	106.5	2±0.1
Roll (deg)	–	6±3	–	11±2	–	10±3
Pitch (deg)	1.5	3±1	20.6	4±2	12.3	4±2
Yaw (deg)	1.3	2±1	11.1	3±2	19.2	4±1

Data for bees are means ± s.d., averaged across all individuals (N=14). For all flight trajectories, only fluctuations above 3 Hz (excluding voluntary, low-frequency motions) are shown.

Assuming nominally similar mean power output in smooth and unsteady flow, the differences in the bees' mean air speed along their flight paths suggests that it would take longer to travel a given distance in unsteady flows (increasing the cost of transport). Though the reduction in mean air speed between smooth and unsteady flow was only ~8%, this difference was consistent between individuals and statistically significant. However, further experiments assessing the flight speeds and metabolic power of bees flying through various intensities and scales of unsteady flow are needed to elucidate the energetic implications of flying in complex aerial environments. If unsteady air flow in the ABL increases energetic costs and/or reduces the mean flight speed of bees, this could have direct implications for the foraging efficiency of bees in natural environments, particularly in windy weather – with potentially adverse effects on colony energetics, growth and pollination efficiency.

Previous work has shown that that fully mixed, turbulent flows have a significant and adverse effect on the flight of orchid bees (Combes and Dudley, 2009). Here, we show that insect flight is also adversely affected by structured, unsteady flows (von Karman vortex streets) emanating from objects. Most interestingly, our results indicate that the orientation of flow structures (vertically *versus* horizontally aligned vortices) has relatively little effect on how instabilities are manifest in flying bees. Our expectation was that a horizontally oriented cylinder (creating a vertical perturbation) would induce variation in pitch angle, whereas a vertically oriented cylinder (creating a lateral perturbation) would induce variation in yaw angle. However, our results clearly demonstrate that in both unsteady flow conditions, bees are most unstable about the lateral/roll axis, and that bees make use of this instability to effect voluntary and corrective maneuvers about this axis as well.

AUTHOR CONTRIBUTIONS

The experiments were performed by S.R. and J.C. All authors equally contributed to conception and design of the experiments and interpretation of the findings being published, and drafting and revising the article.

COMPETING INTERESTS

No competing interests declared.

REFERENCES

Beal, D. N., Hover, F. S., Triantafyllou, M. S., Liao, J. C. and Lauder, G. V. (2006). Passive propulsion in vortex wakes. *J. Fluid Mech.* **549**, 385-402.

Chapman, J. W., Drake, V. A. and Reynolds, D. R. (2011). Recent insights from radar studies of insect flight. *Annu. Rev. Entomol.* **56**, 337-356.

Combes, S. A. and Dudley, R. (2009). Turbulence-driven instabilities limit insect flight performance. *Proc. Natl. Acad. Sci. USA* **106**, 9105-9108.

Crall, J. and Combes, S. (2013). Blown in the wind: bumblebee temporal foraging patterns in naturally varying wind conditions. *Integr. Comp. Biol.* **53**, E270.

Dickinson, M. H., Lehmann, F. O. and Sane, S. P. (1999). Wing rotation and the aerodynamic basis of insect flight. *Science* **284**, 1954-1960.

Diebel, J. (2006). Representing attitude: Euler angles, unit quaternions, and rotation vectors. *Matrix* **58**, 15-16.

Drake, V. A. and Farrow, R. A. (1988). The influence of atmospheric structure and motions on insect migration. *Annu. Rev. Entomol.* **33**, 183-210.

Dudley, R. (2002). *The Biomechanics of Insect Flight: Form, Function, Evolution*. Princeton, NJ: University Press.

Dudley, R. and Ellington, C. P. (1990). Mechanics of forward flight in bumblebees: I. Kinematics and morphology. *J. Exp. Biol.* **148**, 19-52.

Dyhr, J. P., Morgansen, K. A., Daniel, T. L. and Cowan, N. J. (2013). Flexible strategies for flight control: an active role for the abdomen. *J. Exp. Biol.* **216**, 1523-1536.

Ellington, C. P. (1984). The aerodynamics of hovering insect flight. II. Morphological parameters. *Philos. Trans. R. Soc. B* **305**, 17-40.

Ellington, C. P. (1991). Limitations on animal flight performance. *J. Exp. Biol.* **160**, 71-91.

Ellington, C. P., Van den Berg, C., Willmott, A. P. and Thomas, A. L. R. (1996). Leading-edge vortices in insect flight. *Nature* **384**, 626-630.

Feltwell, J. (1982). *Large White Butterfly: The Biology, Biochemistry, and Physiology of Pieris brassicae (Linnaeus)*. The Hague: Dr. W. Junk Publishers.

Hedrick, T. L. (2008). Software techniques for two- and three-dimensional kinematic measurements of biological and biomimetic systems. *Bioinsp. Biomim.* **3**, 034001.

Hedrick, T. L. (2011). Damping in flapping flight and its implications for manoeuvring, scaling and evolution. *J. Exp. Biol.* **214**, 4073-4081.

Heinrich, B. (2004). *Bumblebee Economics*. Cambridge, MA: Harvard University Press.

Hendry, G. (1989). *Midges in Scotland*. Aberdeen, UK: Aberdeen University Press.

Liao, J. C. (2007). A review of fish swimming mechanics and behaviour in altered flows. *Philos. Trans. R. Soc. B* **362**, 1973-1993.

Liao, J. C., Beal, D. N., Lauder, G. V. and Triantafyllou, M. S. (2003). Fish exploiting vortices decrease muscle activity. *Science* **302**, 1566-1569.

Miller, L. A. and Peskin, C. S. (2009). Flexible clap and fling in tiny insect flight. *J. Exp. Biol.* **212**, 3076-3090.

Nicholas, I. K. (2012). *Automated Kinematic Extraction of Wing and Body Motions of Free Flying Diptera*. MSc thesis, University of Maryland, College Park, MD, USA.

Ortega-Jimenez, V. M., Greeter, J. S. M., Mittal, R. and Hedrick, T. L. (2013). Hawkmoth flight stability in turbulent vortex streets. *J. Exp. Biol.* **216** (in press) doi: 10.1242/jeb.089672.

Ristroph, L., Ristroph, G., Morozova, S., Bergou, A. J., Chang, S., Guckenheimer, J., Wang, Z. J., et al. (2013). Active and passive stabilization of body pitch in insect flight. *J. R. Soc. Interface* **10**, 20130237.

Roshko, A. (1961). Experiments on the flow past a circular cylinder at very high Reynolds number. *J. Fluid Mech.* **10**, 345-356.

Sane, S. P. (2003). The aerodynamics of insect flight. *J. Exp. Biol.* **206**, 4191-4208.

Stull, R. B. (1988). *An Introduction to Boundary Layer Meteorology*. Dordrecht: Kluwer Academic Publishers.

Vance, J. T., Faruque, I. and Humbert, J. S. (2013). Kinematic strategies for mitigating gust perturbations in insects. *Bioinsp. Biomim.* **8**, 016004.

Vickery, B. J. (1966). Fluctuating lift and drag on a long cylinder of square cross-section in a smooth and in a turbulent stream. *J. Fluid Mech.* **25**, 481-494.

Walker, S. M., Thomas, A. L. R. and Taylor, G. K. (2012). Operation of the alula as an indicator of gear change in hoverflies. *J R Soc Interface* **9**, 1194-1207.

Wang, Z. J. (2005). Dissecting insect flight. *Annu. Rev. Fluid Mech.* **37**, 183-210.

Watkins, S., Milbank, J., Loxton, B. J. and Melbourne, W. H. (2006). Atmospheric winds and their implications for microair vehicles. *AIAA J.* **44**, 2591-2600.

Willmott, A. P. and Ellington, C. P. (1997). The mechanics of flight in the hawkmoth *Manduca sexta*. I. Kinematics of hovering and forward flight. *J. Exp. Biol.* **200**, 2705-2722.